

Analysis of the transmission and coupling of optical antenna system based on diffraction theory

MIAO HE, PING JIANG, WEINAN CAIYANG, MIAOFANG ZHOU, YAN QIN, BIAO CAO, HUAJUN YANG*
School of Physics, University of Electronic Science and Technology of China, Chengdu 610054, China

Based on diffraction theory, the performance of space optical communication systems consisting of a transmitting antenna, receiving antenna, and fiber coupling system is analyzed in detail. Besides, several practical situations are also involved such as antenna defocus and fiber deviation. According to the simulation results, defocusing on the primary mirror will improve the transmission efficiency and coupling efficiency of the system in some cases. Coupling efficiency can be increased by 15.57%; when the primary mirror of the antenna is defocused, the coupling efficiency can be increased by 15.31% by adjusting the position of the optical fiber.

(Received June 4, 2021; accepted April 8, 2022)

Keywords: Space optical communications, Fiber coupling efficiency, Optical antenna system

1. Introduction

Free-space optical communication has the advantages of large communication bandwidth, large channel capacity, and large optical gain. It is one of the technical solutions to realize high-speed and large-capacity communication and is widely used in various fields [1-4]. The stable interconnection and high coupling efficiency between the laser beam and the single-mode fiber are the prerequisites for improving the transmission capacity and fidelity, and it is also an important link in free-space optical communication. Therefore, laser coupling transmission technology has been an attractive field for quite a long time [5-17].

Many researchers focus on fiber coupling systems to improve coupling efficiency. They are keen to add one or more optical elements between the fiber and the laser beam to shape the spot so that the energy entering the fiber end face is as high as possible. Researchers have designed spherical mirrors [5], semi-cylindrical mirrors [6], and other lenses [7] to improve the coupling efficiency of the system. Design and use the coupling system of the lens group to reduce the influence of fiber position deviation [8-13]. An optical system with a concave lens and a set of positive-negative angular cone lenses is designed to change the hollow beams with different hollow ratios into solid beams, and the coupling efficiency can be improved to the optimum value of 0.808. [12]. In addition, the researchers also considered designing micro-lens fibers, that is, attaching specific micro-lens to the end face of a single-mode fiber

[14,15], or designing the fiber collimator to improve the coupling efficiency [16,17]. These designs can greatly improve the coupling efficiency of the system, but they separate transmission and coupling and do not put it into the entire communication system for analysis. Optical fiber coupling is a part of free space communication and occupies an important position in the entire antenna transmission system. The literature [18] combined the coupling system with the optical antenna system and used the geometric optical analysis method. Based on the vector refraction theory, a 3D ray-tracing method is used to calculate the space light transmitted through a complex optical system. Although this method is convenient for programming and simulation, it ignores the diffraction effect of the beam during transmission, which will cause calculation errors to a certain extent. At present, we have hardly seen the use of diffraction theory to analyze the transmission and coupling of the entire system.

This paper uses diffraction theory to analyze the entire system, including the transmission and coupling of the system. This paper also introduces the defocus of the antenna, analyzes the effect of antenna defocus on fiber coupling, and proposes an optimization scheme to improve the coupling efficiency based on the simulation results.

2. Theoretical method

Diffraction theory will be used to analyze a traditional Cassegrain antenna system shown in Fig. 1.

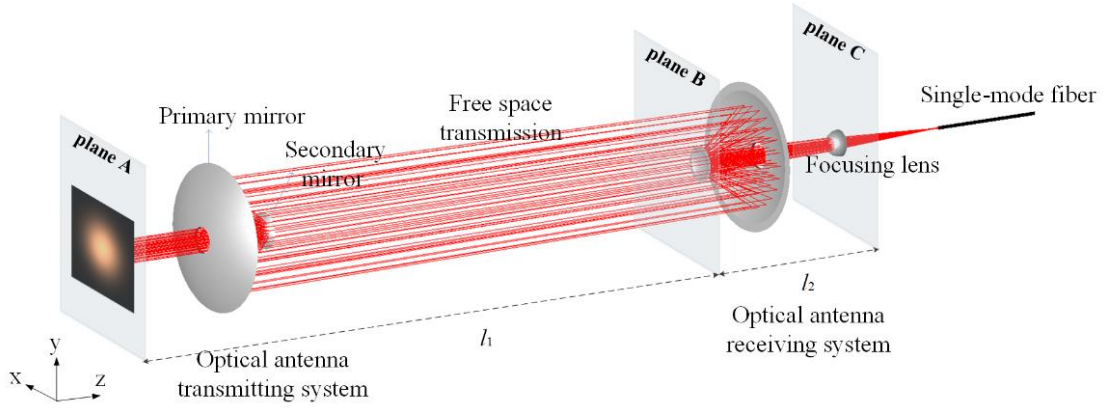


Fig.1. Schematic diagram of Cassegrain optical antenna transmission system. Plane A is placed in front of the transmitting antenna, plane B is placed in front of the receiving antenna, and plane C is placed on the front surface of the lens (color online)

The Gaussian beam at the initial plane ($z=0$) can be expressed as [19]

$$E_{in}(x_1, y_1) = \exp\left[-(x_1^2 + y_1^2)/w_0^2\right] \quad (1)$$

The complex amplitude of the beam arriving at receiving plane B can be expressed by the generalized Collins formula [20]

$$E(x_2, y_2) = -\frac{j}{\lambda B} \iint E_{in}(x_1, y_1) \exp[jkw(x_1, y_1, x_2, y_2)] dx_1 dy_1 \quad (2)$$

$$w(x_1, y_1, x_2, y_2) = L_0 + (1/2B)[A(x_1^2 + y_1^2) - 2(x_1x_2 + y_1y_2) + D(x_2^2 + y_2^2)] \quad (3)$$

where k is the wavenumber, L_0 is the optical path of the input and output fields along the optical axis. A, B, C and D are the parameters for the ABCD transmission matrix of the optical antenna.

It is worth noting that, although the apertures of the transmitting antenna and the receiving antenna are the same, the whole system still cannot be expressed in one ABCD matrix and the Collins formula has to be used twice to obtain a more accurate result. The reason can be simply described as that, for long-distance propagation, the diffraction definitely reshapes the optic field so that the integrand of the Collins formula at plane B should be rewritten.

Therefore, the matrix of the transmitting system and the receiving system will be given separately.

The transmission matrix of the transmitting antenna can be expressed as [21]

$$T(\delta_1) = \begin{pmatrix} \frac{f_1^2 - (f_1 - l_1)\delta_1}{f_1 f_2} & \frac{f_2(l_1 - f_1)}{f_1} \\ \frac{\delta_1}{f_1 f_2} & \frac{f_2}{f_1} \end{pmatrix} \quad (4)$$

According to the derivation method of $T(\delta_1)$, the transmission matrix of the receiving optical antenna can be expressed as

$$T(\delta_2) = \begin{pmatrix} 1 & l_2 \\ 0 & 1 \end{pmatrix} \begin{pmatrix} 1 & 0 \\ \frac{1}{f_2} & 1 \end{pmatrix} \begin{pmatrix} 1 & f_1 - f_2 - \delta_2 \\ 0 & 1 \end{pmatrix} \begin{pmatrix} 1 & 0 \\ -\frac{1}{f_1} & 1 \end{pmatrix} \begin{pmatrix} 1 & f_1 \\ 0 & 1 \end{pmatrix} \\ = \begin{pmatrix} \frac{f_2^2 + (f_2 + l_2)\delta_1}{f_1 f_2} & \frac{f_1(l_2 + f_2)}{f_2} \\ \frac{\delta_2}{f_1 f_2} & \frac{f_1}{f_2} \end{pmatrix} \quad (5)$$

where f_1 and f_2 are the primary and the secondary mirrors' focal lengths, respectively. Because of the influence of heat and vibration, axial defocus always appear in the Cassegrain antenna system. Here we define δ_1 as the axial defocus of the primary mirror of the transmitting antenna, and δ_2 is the axial defocus of the primary mirror of the receiving antenna. The movement of the transmitting primary mirror in the positive direction of the z-axis is expressed as $\delta_1 > 0$, otherwise $\delta_1 < 0$. The movement of the receiving primary mirror in the positive direction of the z-axis is expressed as $\delta_2 < 0$, otherwise $\delta_2 > 0$. The primary mirror defocus model diagram is shown in Fig. 2.

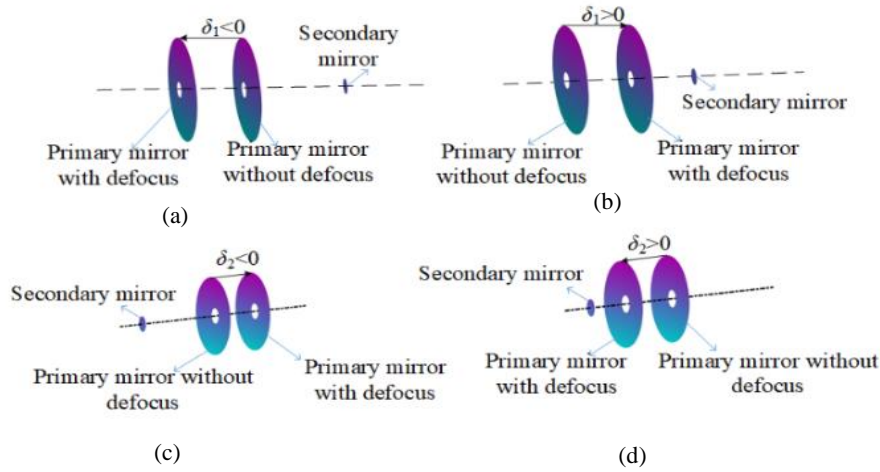


Fig. 2. Defocus of the primary mirror in the transmitting system: (a) (b) and in the receiving system: (c) (d) (color online)

As an important parameter to measure system performance, the coupling efficiency of the antenna can be expressed as [22]

$$\eta = \frac{\left| \iint E_{out} E_s^* ds \right|^2}{\iint |E_{out}|^2 ds \iint |E_s|^2 ds} \quad (6)$$

where E_{out} and E_s are the mode field of the beam in the coupling plane and the mode field of the fiber.

3. Discussion and analysis

In order to study the transmission of the beam in the system, we selected the parameters for simulation analysis: $f_1=300$ mm, $f_2=60$ mm, the distance between the primary mirror and secondary mirror is 240 mm, $\omega_0=10$ mm, $\lambda=1550$ nm.

3.1. System transmission

The antenna system without defocusing still has to suffer from diffraction loss. Diffraction loss is mainly composed of two parts: secondary mirror occlusion loss and primary mirror truncation loss. The blocking loss of the secondary mirror is caused by the blocking of the diffracted energy by the receiving secondary mirror, and the truncation loss of the primary mirror is caused by the energy leakage at the periphery of the receiving primary mirror.

Fig. 3(a) shows the relationship between the transmission distance, transmission efficiency, and transmission loss. As shown in Fig. 3(a), as the transmission distance increases, the transmission efficiency decreases, the truncation loss of the primary mirror increases and the blocking loss of the secondary mirror first increases and then decreases. Mark point A and point B for analysis. According to Eq. (2), we draw the diffraction field pattern on plane B when $l_1=1000$ m and $l_1=5000$ m, as shown in Fig. 3(b) and Fig. 3(c). The white circle in the figure indicates

the boundary of the receiving antenna reflector. It can be seen that when $l_1=5000$ m, the area of the spot distribution is larger, the energy of the central part is reduced, the energy beyond the receiving range of the primary mirror increases, and the overall diffraction loss increases. Therefore, it can be seen that as the transmission distance increases, the influence of diffraction becomes greater.

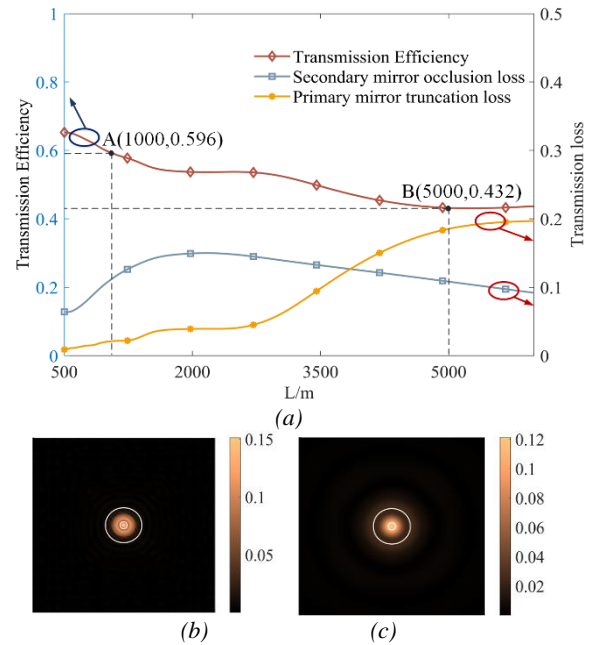


Fig. 3. (a) Relationship between the transmission distance, transmission efficiency, and transmission loss. (b) Diffraction pattern on plane B when $l_1=1000$ m. (c) Diffraction pattern on plane B when $l_1=5000$ m. The white circle on the diffraction pattern indicates the edge of the primary mirror and the secondary mirror of receiving antenna (color online)

Fig. 4 shows the relationship between the defocus distance of the transmission primary mirror, transmission efficiency, and transmission loss when $l_1=1000$ m. It can be seen that the defocus distance has a great influence on transmission efficiency and transmission loss. We can see

that when $\delta_1 > 0$, the transmission efficiency curve has a downward trend. This is because the ray emitted from the transmitting antenna in this state is divergent. As δ_1 increases, the divergence angle becomes larger, and the receiving antenna receives less energy. However, when $\delta_1 < 0$, the curve fluctuates, and the transmission efficiency has two extreme values. Through analysis, it can be known that when $\delta_1 < 0$, the emitted rays first converge and then diverge. And as the absolute value of δ_1 increases, the ray convergence point gets closer to the transmitting antenna. In the process from point C to point D, the ray converges to the receiving secondary mirror, and the occlusion loss of the secondary mirror increases. It can be seen from Fig. 4 that the occlusion loss of the receiving secondary mirror is the largest at point D, which means that the secondary mirror of the receiving antenna is exactly at the convergence point of the rays. As the absolute value of δ_1 increases from point D, the convergent rays start to be divergent, so the transmission efficiency first increases and then decreases.

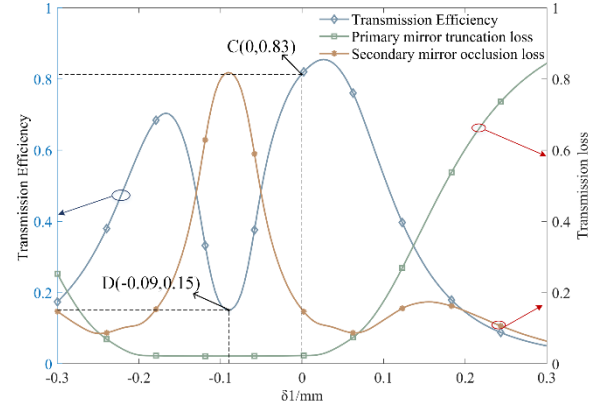


Fig. 4. Relationship between the defocus distance of the transmission primary mirror, transmission efficiency and transmission loss when $l_1=1000$ m (color online)

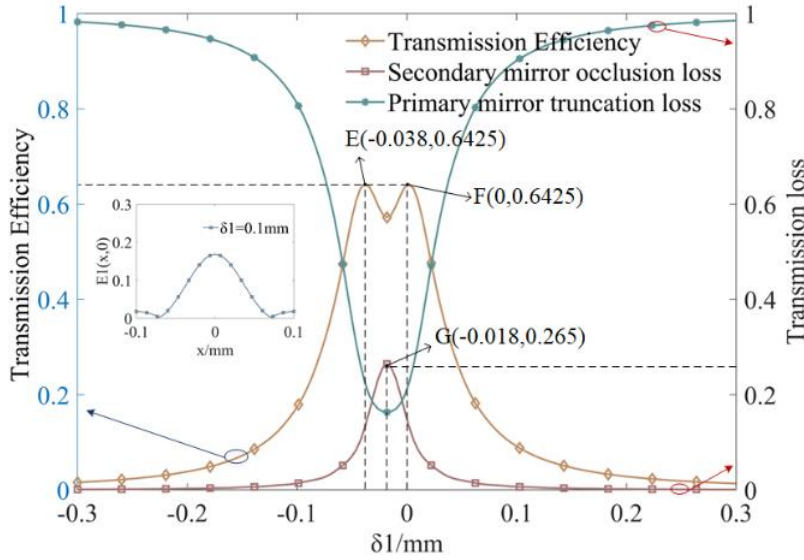


Fig. 5. Relationship between the defocus distance of the transmission primary mirror, transmission efficiency and transmission loss when $l_1=5000$ m. The small graph is the distribution graph of the amplitude value of point G (color online)

Fig. 5 shows the relationship between the defocus distance of the transmission primary mirror, transmission efficiency, and transmission loss when $l_1=5000$ m. It can be seen from the distribution of the transmission efficiency curve that $\delta_1=0$ is not the only maximum point. Marking points E and F are the places where the transmission efficiency is maximum. The occlusion loss of the secondary mirror is the largest at point G. It can be seen from the amplitude value curve of point G that the energy is concentrated in the central area, but the spot area is larger than the area blocked by the receiving secondary mirror, so it can still receive part of the energy. The increase in transmission efficiency at point E and point F can be explained by the curve change in Fig. 5. The reduction in the blocking loss of the secondary mirror is greater than the increase in the truncation loss of the primary mirror, so the transmission efficiency increases.

3.2. Coupling efficiency

The coupling of the beam and fiber requires mode field matching. Therefore, the diffraction field after the beam passes through the system needs to be calculated. According to Parseval's theorem, the coupling efficiency can be calculated directly on the receiving plane, and the reverse transmission from the fiber mode field to the receiving plane can be expressed as [23]

$$F_A = \sqrt{\frac{2}{\pi w_A^2}} \exp \left\{ - \left(\frac{1}{w_A^2} - j \frac{\pi \Delta z}{\lambda f^2} \right) \times \left[(x - \Delta \varphi_x f)^2 + (y - \Delta \varphi_y f)^2 \right] \right\} \times \exp \left\{ j 2\pi \left[\frac{\Delta x}{\lambda f} (x - \Delta \varphi_x f)^2 + \frac{\Delta y}{\lambda f} (y - \Delta \varphi_y f)^2 \right] \right\} \quad (7)$$

where f is the focal length of the lens, w_A is the mode-field radius of the backpropagated fiber mode, given by $w_A = \lambda f / (\pi w_f)$, w_f is the mode field radius of single-mode fiber. Δx and Δy are the lateral offset of the fiber axis relative to the x -axis and y -axis. $\Delta \phi_x$ and $\Delta \phi_y$ is the inclination angle of the optical fiber in the xz plane and the yz plane. Δz are the defocus of the fiber lens system.

Assuming $l_1=1000$ m, use Eq.(6) to calculate coupling efficiency. Fig. 6(a) is the relationship between the defocus distance of the primary mirror and the coupling efficiency. Fig. 6(b) is the top view of Fig. 6(a). It can be seen that the defocus of the primary mirror has a significant impact on the coupling efficiency. Mark point H, the receiving

antenna and the transmitting antenna without defocusing, and the coupling efficiency is 47.31%. Mark point I as the highest coupling efficiency point in Fig. 6(b), the primary mirror of the transmitting antenna moves to the left, and the primary mirror of the receiving antenna moves to the left, and the coupling efficiency reaches 62.88%. Compared to the state at point H, the coupling efficiency at point I increased by 15.57%. The reason for this phenomenon may be that the shifting of the receiving primary mirror adjusts the distribution of the light beam at the receiving plane so that the receiving field and the mode field of the fiber match better and the coupling efficiency increases.

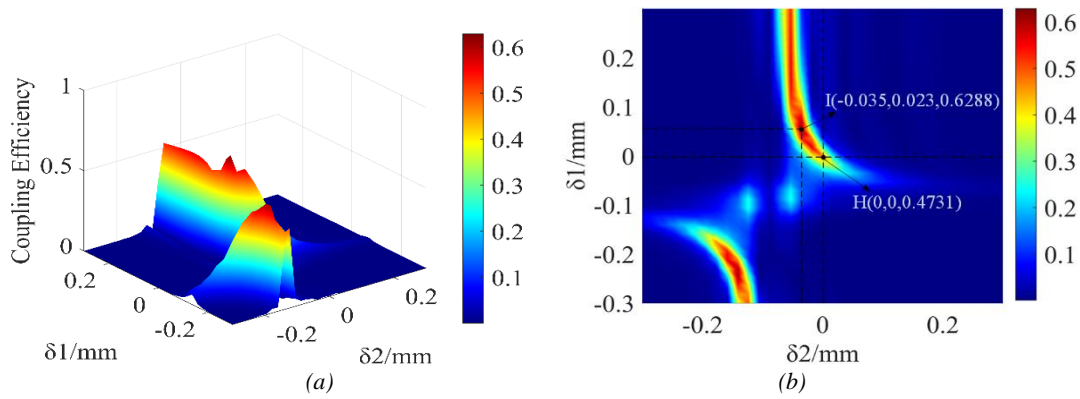


Fig. 6.(a) Relationship between the defocus distance of the primary mirror and the coupling efficiency. (b):Top view of (a) (color online)

It can be seen from the distribution diagram of coupling efficiency in Fig. 6(b) that if the transmitting primary mirror and the receiving primary mirror are moved to an appropriate position, the coupling efficiency can be effectively improved. The analysis can conclude that when $\delta_1 > 0$, $\delta_2 < 0$, and $\delta_1 < 0$, $\delta_2 < 0$, the beam will converge after passing through the receiving antenna. Theoretically, when the receiving plane is at a reasonable position, the matching degree of the beam and the optical fiber will increase. It can be seen from Fig. 6(b) that there is an increase in coupling efficiency in these two regions. This can be used as an optimization scheme to improve transmission efficiency and provide new ideas for some engineering designs. However, from Fig.4 and Fig. 5, we can see that the offset

of the transmitter's primary mirror has an obvious effect on the transmission efficiency. If you use this method to improve the coupling efficiency, you must accept the lower system transmission efficiency.

In actual situations, when the optical fiber is coupled with the beam, the position of the optical fiber may change due to the influence of external factors, which will have a great impact on the coupling efficiency. The movement of fiber position generally considers three situations: defocus Δz of the fiber–lens system, lateral offset of the fiber, and deflection angle of the fiber. We simulated the relationship between fiber position movement and coupling efficiency, as shown in Fig. 7.

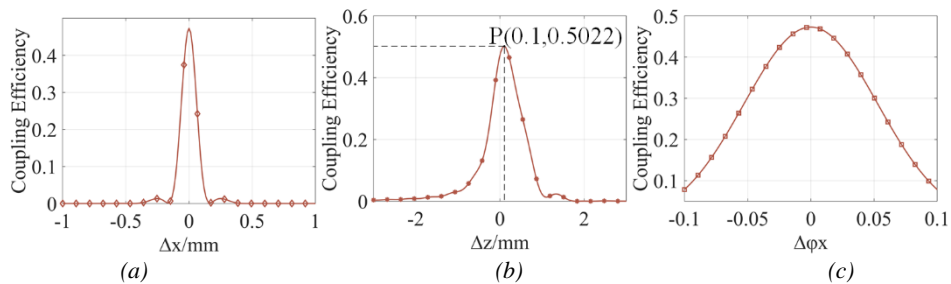


Fig. 7. (a) Relationship between the lateral offset of the fiber and the coupling efficiency. (b) Relationship between the defocus Δz of the fiber–lens system and the coupling efficiency. (c) Relationship between the deflection angle of fiber and the coupling efficiency (color online)

It can be seen from the variation curve of the coupling efficiency in Fig. 7 that when the fiber has lateral defocus or the fiber has a deflection angle, the coupling decreases. However, when the defocus Δz of the fiber lens system is small, the coupling efficiency will increase slightly, reaching 50.22%.

When $\Delta z=0$, the coupling efficiency is 47.31%. It can be seen that the existence of a small amount of defocus Δz can increase the coupling efficiency by 2.91%.

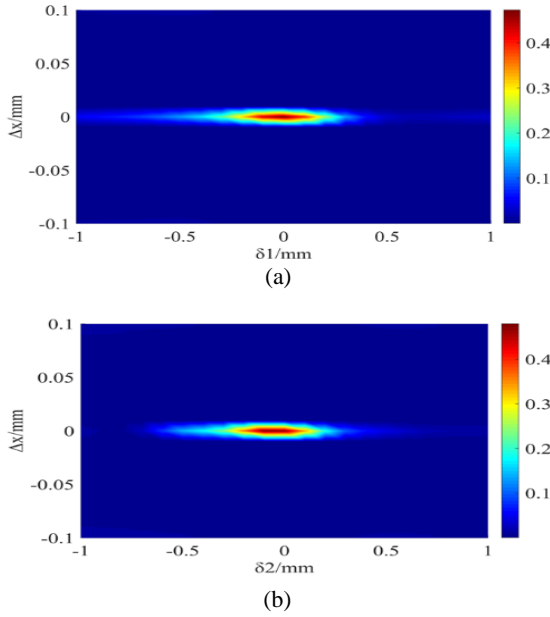


Fig. 8.(a)Relationship between the defocus distance of the transmitting primary mirror, lateral offset of the fiber, and the coupling efficiency. (b) Relationship between the defocus distance of the receiving primary mirror, lateral offset of the fiber, and the coupling efficiency. Color bars indicate coupling efficiency (color online)

According to Eqs. (2), (6), and (7), we calculated the coupling efficiency of the primary mirror defocus system when the optical fiber is moved. Since the movement of the fiber in the x-direction has the same result as the movement in the y-direction, we only simulate the movement of the fiber in the x-direction. Fig. 8 shows the relationship between the defocus of the primary mirror, lateral offset of fiber, and the coupling efficiency.

It can be seen from Fig. 8(a) and Fig. 8(b) that the coupling efficiency of the system is the highest under ideal conditions. The coupling efficiency is symmetrical and gradually decreases on both sides of $\delta_{1,2}=0$ and $\Delta x=0$. It is worth noting that, compared with the defocus amount $\delta_{1,2}$ of the primary mirror, the fiber offset has a greater impact on the coupling efficiency. Therefore, precise focusing of optical fibers is particularly important in engineering applications.

It can be seen from Fig. 9(a) and Fig. 9(b) that when the absolute value of the change $\Delta\phi_x$ of the fiber deflection angle on the xz plane is the same, the coupling efficiency is the same. When determining the offset distance of the primary mirror, the deflection angle of the fiber will reduce the coupling efficiency. This is consistent with the results of previous studies. In an actual system, it is difficult to

ensure that the optical fiber and antenna do not shift. Therefore, both the primary mirror and the optical fiber are allowed to have smaller deviations, which can reduce the difficulty of operation.

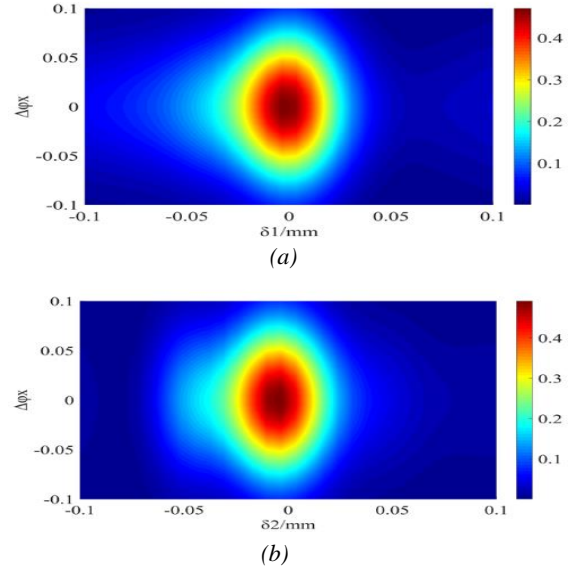


Fig. 9. (a) Relationship between the defocus distance of the transmitting primary mirror, deflection angle of fiber, and the coupling efficiency; (b) Relationship between the defocus distance of the receiving primary mirror, deflection angle of fiber, and the coupling efficiency. Color bars indicate coupling efficiency (color online)

Fig. 10 shows the relationship between the defocus of the primary mirror, defocus Δz of the fiber–lens system, and the coupling efficiency.

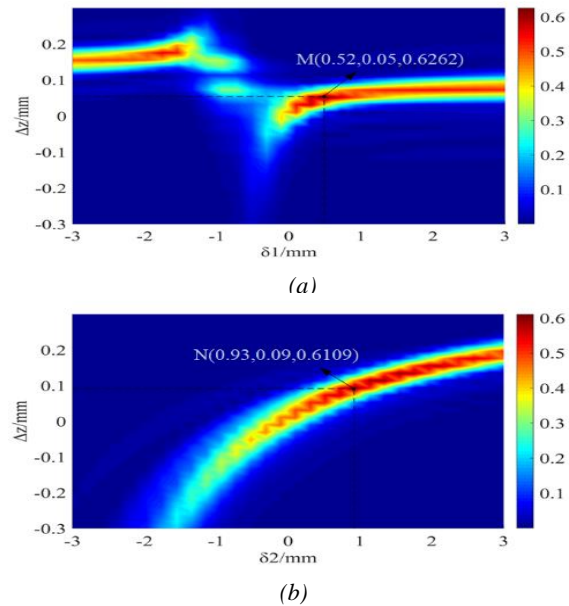


Fig. 10. (a)Relationship between the defocus distance of the transmitting primary mirror, defocus Δz of the fiber–lens system, and the coupling efficiency. (b)Relationship between the defocus distance of the receiving primary mirror, defocus Δz of the fiber–lens system, and the coupling efficiency. Color bars indicate coupling efficiency (color online)

An interesting phenomenon appears in the picture at this time. The coupling efficiency under ideal conditions is not the highest. When the antenna mirror and the optical fiber are offset at a certain distance at the same time, the coupling efficiency has been significantly improved. Fig. 10 shows the data of point M and point N. When $\delta_1=0.52$ mm, $\Delta z=0.05$ mm, the coupling efficiency is 62.62%, and the coupling efficiency is increased by 15.31%. When $\delta_2=0.93$ mm, $\Delta z=0.09$ mm, the coupling efficiency is 61.09%, and the coupling efficiency is increased by 13.78%. The reason for this phenomenon may be that the movement of the transmission primary mirror changes the field distribution at the coupling plane. The movement of the fiber can be regarded as a kind of adjustment, which increases the matching degree of the fiber mode field and the light field, and increases the coupling efficiency.

This scheme of improving the coupling efficiency by adjusting the antenna primary mirror and the amount of optical fiber defocus is relatively simple and feasible. Without considering the transmission efficiency, we can deliberately introduce the defocus of the primary mirror and then adjust the position of the fiber to improve the coupling efficiency.

4. Conclusion

Based on diffraction theory, the performance of space optical communication systems consisting of a transmitting antenna, receiving antenna, and fiber coupling systems are analyzed in detail. Besides, several practical situations are also involved such as the defocus of the antenna and the deviation of the fiber. The simulation results show that as the transmission distance increases, the influence of diffraction becomes greater. When $\delta_1=0.023$ mm and $\delta_2=-0.035$ mm, the coupling efficiency is 62.88%, and the coupling efficiency is increased by 15.57%. When the primary mirror of the antenna is defocused, the coupling efficiency can be increased by 15.31% by adjusting the position of the fiber. The conclusions presented in this paper will provide meaningful information for engineers engaged in space optical communications.

Acknowledgements

This work was supported by National Natural Science Foundation of China (NSFC) (11574042, 61271167).

References

- [1] D. R. Kolev, M. Toyoshima, *J. Lightwave Technol.* **35**, 103 (2017).
- [2] L. Zhang, J. S. Dai, C. K. Li, J. C. Wu, J. J. Jia, J. Y. Wang, *Opt. Express* **28**, 8291 (2020).
- [3] D. Liu, Y. D. Zhou, W. B. Chen, Q. Liu, T. Y. Huang, W. Liu, Q. K. Chen, Z. P. Liu, P. T. Xu, X. Y. Cui, X. B. Wang, C. F. Le, C. Liu, *Opt. Express* **27**, A654 (2019).
- [4] M. Zhao, C. B. Xie, Z. Q. Zhong, B. X. Wang, Z. Z. Wang, P. D. Dai, Z. Shang, M. Tan, D. Liu, Y. J. Wang, *J. Opt. Soc. Korea* **19**, 695 (2015).
- [5] F. Zhang, Y. Zheng, S. Q. Lu, *Optik* **157**, 497 (2018).
- [6] J. Sakai, T. Kimura, *IEEE J. Quantum Electron* **16**, 105980.
- [7] M. Thual, P. Chanclou, O. Gautreau, *Electron. Lett.* **39**, 1504 (2003).
- [8] M. N. Hasan, M. U. Haque, Y. C. Lee, *Opt. Eng.* **55**, 9 (2016).
- [9] M. Fadhali, J. Zainal, Y. Munajat, *Optik* **120**, 384 009).
- [10] J. D. Mao, H. J. Sheng, C. Y. Zhou, *J. Russ. Laser Res.* **33**, 186 (2012).
- [11] A. Heinrich, C. Hagen, B. Nussbaumer, California, USA, p. 0W1, 2014.
- [12] B. Cao, H. J. Yang, P. Jiang, *Optics Communications* **493**, 127029 (2021).
- [13] W. Song, Y. J. Xie, Z. G. Li, W. Hao, P. P. Yan, X. Li, *Proc. SPIE* **11780**, 11781E (2021).
- [14] H. M. Yang, C. T. Chen, R. Ro, *Opt. Laser Technol.* **42**, 918 (2010).
- [15] R. A. Modavis, T. W. Webb, *IEEE Photonics Technology Letters* **7**, 7 (1995).
- [16] S. Bondarenko, M. Hülsemann, A. Mai, P. Steglich, *Opt. Eng* **60**, 014105 (2021).
- [17] Q. Q. Kong, Y. Q. Jing, H. Shen, S. W. Deng, Z. G. Han, R. H. Zhu, *Chinese Optics Letters* **18**, 021402 (2020).
- [18] P. Jiang, H. J. Yang, and S. Q. Mao, *Opt. Express* **23**, 26104 (2015).
- [19] J. J. Zhang, P. Jiang, H. J. Yang, W. N. Caiyang, B. Cao, Y. Niu, M. J. Wang, *Appl. Opt.* **59**, 7567 20).
- [20] Z. Yang, *Optik* **125**, 3181 (2014).
- [21] M. Y. Yu, H. J. Yang, P. Jiang, Y. Zhang, L. Chen, *Optik* **127**, 1734 (2016).
- [22] W. J. Chen, H. J. Yang, Z. B. Li, J. Li, B. Zhu, *Optik* **121**, 2259 (2010).
- [23] O. Wallner, P. J. Winzer, W. R. Leeb, *Appl. Opt.* **41**, 637 (2002).

* Corresponding authors: yanghj@uestc.edu.cn